Molecular dynamics simulations of the self-diffusion of monodisperse chains oligomers and of their trace diffusion in an entangled polymer host.

M. Durand, H. Meyer,* and J. Baschnagel
Institut Charles Sadron, CNRS, 23 rue du Loess–BP 84047, 67034 Strasbourg Cedex 2, France

O. Vitrac†
UMR Génie industriel alimentaire, AgroParisTech site de Massy, 1 avenue des Olympiades, 91744 Massy Cedex, France

The apparent analogy between the self-diffusion of linear oligomers, 2 up to 64 monomers, and their trace diffusion in an entangled polymer host of length 256 was investigated by molecular dynamics at constant pressure. Oligomers and polymers were represented by a same generic coarse-grained (bead-spring) model. The scaling relationships of the self-diffusion coefficient, D, and trace diffusion coefficient, D_T, with the chain length, N, of the diffusant, written as $D \propto N^{-\alpha}$ and $D_T \propto N^{-\alpha}$, were analyzed for a wide range of temperatures down to the glass transition temperature, T_g. Near T_g, the heterogeneous dynamics was assessed by the self part of the van-Hove distribution function and non-Gaussian parameters. For both self-diffusion and trace diffusion, a scaling obeying to $\alpha = 1$ was identified at all temperatures and regardless of the oligomer lengths. [to be continued]

I. INTRODUCTION

In many technological areas, understanding the molecular diffusion mechanism in polymer materials is of significant concern in both qualitative and quantitative ways. The diffusion and rheological properties of linear and branched polymers depend on the scaling relationship of the polymer self-diffusivity and viscosity with molecular weight [10]. In formulated materials such as common polyolefins and polystyrenes, tracer diffusion controls the loss of additives and consequently the life-time of the processed material or the contamination of materials in contact (e.g. food, environment) [17]. In this perspective, the development of predictive models of the diffusion coefficients of tracers could help the design of safer materials [14] and the assessment of consumer exposure to contaminants originating from polymer materials [16]. For both self-diffusion coefficients of polymer segments and tracer diffusion coefficients of dispersed solutes (e.g. additives, polymer residues), the dependence between the molecular mass of the diffusing species (M), its size or length in fact, and its diffusion coefficient, D must be elucidated. For linear molecules, several theories have been successfully related to experimental scaling relationships, such as $D \propto M^{-\alpha}$ with a scaling exponent denoted α. The reptation model involving $\alpha = 2$ predicts that very long chains in concentrated solutions or melts are constrained by their neighboring intertwined chains and that they can therefore diffuse only along their own contours. Literature data in melts were found consistent with $\alpha = 2.3$ [10] based on rheological measurements or $\alpha = 2.4$ [19] based on diffusion coefficients measurements with pulsed-field gradient nuclear magnetic resonance. The discrepancies between the model and experiments have been related to additional mechanisms including erosion, as inferred by neutron spin echo, [20] or fluctuations[3] of the virtual tube confining the diffusing molecule. For chains that are significantly shorter than the entanglement length, the random walk of the center-of-mass of the diffusing species is expected to be controlled by the balance between friction/viscous forces and entropic forces on each sub-unit. When the fluctuations of each sub-unit are independent, a scaling exponent $\alpha = 1$ is foreseen as predicted in the Rouse model[13]. Experimental data showed the molecular mass dependence was stronger than the one predicted with the Rouse theory with α values greater than 1 and that vary with the considered temperature and pressure. In liquid n-alkanes ranging between 8 and 60 carbons, Meerwall et al. [18] found values from 2.72 down to 1.85 when temperature was changed from 30 to 170℃, and with the special case $\alpha = 2$ obtained at 130℃. It was shown that experimental results could be reconciliated with Rouse theory a posteriori after a correction due to the excess free volume of chain ends. [18]. The geometric effect of free volumes was investigated for C_{60} and the thermal dependence of α was reproduced by molecular dynamics (MD) simulations for alkanes ranging between C_{16} and C_{60} [5]. Long term atomistic MD simulations of polyethylene melts led to the identification of a Rouse regime for chain lengths ranging approximately between C_{90} a C_{140} at 450K.[6]. For small tracer molecules dispersed at very low concentration in a host matrix of much longer chains, the possible variety of scaling exponents is also large. In semi-crystalline polyolefins, α values much greater than 1 were found for additive-like molecules[9], with values ranged between 1.6 and 4 for temperatures ranging between 23℃ and 40℃, and for linear alkanes (between C_{12} and C_{18}), with values close to 2, [15]. A similar range between 2 and 4.7 for temperatures ranging from 23 to 85 ℃ was obtained in a lightly crosslinked

*Corresponding author: hmeyer@ics.u-strasbg.fr
†Corresponding author: olivier.vitrac@agroparistech.fr

amorphous polyamide around or above its glass transition temperature T_g .[8]. For rigid tracers such as fluorophores, dynamics highly heterogeneous in space and in time were identified around the transition temperature [2],[1] and up to 100K above T_g [11]. The persistence of correlated motions or trapped states was consequently proposed to explain the wide spread of values with the size, the shape and stiffness of diffusants in conditions of use of polymers[14]. By contrast, in polyethylene melts at 180℃, an α value close to 1 was inferred for n-alkanes (between C_{24} and C_{60}) after extrapolation of mutual diffusion coefficients at infinite dilution.

Confronted with this whealth of partly contradicting results, the aim of this paper is to clarify the scaling relation $D \propto M^{-\alpha}$ for one of the simplest possible models in MD simulations.

From the mechanistic point of view, the comparison between the scaling relationship of D with M for polymer host and tracer diffusants is particularly interesting when both molecules are chemically close and differ only from their size. By fixing the length of polymer host to a value larger than the diffusant (i.e. the bulk density is constant) in MD simulations, the effect of tracer diffusant length can be investigated without additional biases due to free volume effects. The only price to pay is that the expected statistics relying on isolated molecules (e.g. bidisperse system) is poorer than for much larger ensembles. In this perspective, the current work is the first part of a series of two papers aiming at assessing via MD simulations the scaling relationships of D with M for monodisperse and mixtures of linear polymers. In order to explore a wide range of lengths and temperatures from high temperatures down to polymer T_g , a purely repulsive coarse-grained model (bead-spring) was considered. As each bead can move freely without torsional constraints, the simulated polymer is not crystallizable and the assumption of heterogeneous dynamics at low temperature can be tested. In addition, it is argued that the introduction of an almost exchangeability property between connected and non-connected beads may reduce the need of subsequent corrections due to excess volumes at chain ends and would make it possible to assess theoretically the cross-over between a Rouse regime towards an entangled regime. The first paper presents the scaling relationship of self-diffusion coefficients in oligomers consisting of two beads up to their entanglement length (32 beads) and the scaling relationship of self-diffusion coefficients of similar size (from 2 to 32 beads) in a matrix of 256 beads. The possible symmetry between the roles of the host and of the guest is in particular discussed on a wide range of temperature. The related thermodynamical interpretation as activation energy and volume and the detailed relaxation of the different Rouse modes are detailed in a companion paper. The paper is organized as follows. The simulation procedure is detailed in section II. The main properties of the Rouse theory are summarized in section III along the statistical criteria used to test the theory. The results above T_g and in vicinity of T_g are presented in section IV. The increasing role of heterogeneous dynamics on diffusion coefficients when the temperature is decreased down to T_g is particularly highlighted. Finally, in the last section summarizes the main findings and sketches future work.

II. SIMULATION DETAILS

A. MODEL

Oligomer and polymer segments were idealized at a coarse-grained scale as a flexible, non-crystallizable, bead-spring models. Interactions between non-bonded monomers were represented by a truncated and shifted Lennard-Jones (LJ) potential with a cut-off radius corresponding to the minimum of the LJ potential.

$$U_{\text{L-J}}^{\text{rep}} = \begin{cases} 4\epsilon \left[\left(\frac{\sigma}{r}\right)^{12} - \left(\frac{\sigma}{r}\right)^{6} + \frac{1}{4} \right] & \text{for } r \leq r_{\min} \ , \\ 0 & \text{else.} \end{cases} \tag{1}$$

All quantities were expressed in dimensionless LJ units. In this framework, lengths energies and temperatures are scaled by σ(monomer diameter), ϵ and ϵ/k_B. For convenience, the Boltzmann constant k_B was set equal to 1. Time scale was finally expressed as $\tau = (m\sigma^2/\epsilon)^{1/2}$. Along the polymer chain, connected monomers were not subjected to a LJ potential but to a harmonic potential instead:

$$U_{\text{bond}}(r) = \frac{1}{2} k (r - r_0)^2 \ . \tag{2}$$

The value $r_0 = 0.967$ acted as the average bond length between two monomers. As r_0 was lower than one, bonded monomers tended to slightly overlap. The spring stiffness $k = 1111$ was chosen large enough to prevent chains from crossing each other. The incommensurability between the lengths imposed by the harmonic and the LJ potentials impeded crystallization on cooling. The generated model was very flexible as back folding was only prevented by the LJ potential. The minimum angle between two neighboring bonds was approximately 70 °.

B. SYSTEMS

Two types of dispersions systems were considered: monodisperse linear systems consisting in 3072 beads and polydisperse linear systems consisting in 12288 beads. As in our coarse-grained model, a bead/monomer had a unitary molecular mass, the molecular mass of each linear diffusant was determined by its number of beads, N, ones. Oligomers of length $N = 2(1536), 4(768), 8(384), 16(192), 32(96), 64(48)$ were considered in monodisperse systems, where the figure in parenthesis represents the number

of chains. Tracer diffusants had a similar size length than monodisperse systems. Two sets were considered, $N = 1(8), 2(4), 4(4), 16(4)$ and $N = 1(8), 2(4), 4(4), 8(4), 16(4), 32(4), 64(4)$, which were included in a matrix of size 64 and 256 respectively. For both sets, the achieved concentrations in tracers, ranging from 1 to 4%, was enough low to prevent a significant plasticization of the host matrix.

C. SIMULATION PROCEDURE

The equations of motion corresponding to the considered pair forcefields were integrated using the velocity-Verlet algorithm with a time step of $\delta t = 0.01$. Simulations were performed under isothermal and isobaric conditions (NpT ensemble) using a Langevin thermostat and a Berendsen barostat. The friction coefficient of the thermostat was set to $\gamma = 0.1$ and the coupling parameter of the barostat to $\tau_{\rm p} = 1 \times 10^{-5}$. The initial configuration with an initial density of $\rho = 0.85$ [7] was equilibrated in the NpT statistical ensemble at $T = 1.0$ and $p = 5.0$ during $\tau_{\rm e} = 22000\tau$, which was comparable to the relaxation of the longest chain (squared end-to-end distance correlation time of about $22 \times 10^3\tau$). The obtained configuration was used as starting configuration for all subsequent long-term simulations at $T = 1.0$ or at lower temperatures. The absence of ageing was verified by ensuring that all chains could translate on distances larger than their square end-to-end distance $R_{\rm e}^2$. Configurations at lower temperatures were obtained by cooling the starting configuration from $T = 1.0$ down to the desired temperature at constant pressure with a cooling rate of $\Gamma_{\rm T} = 2 \times 10^{-5}$. The obtained configuration was subsequently equilibriated as previously described for $T = 1.0$. Long term simulations were finally performed for each temperature until the self-diffusive regime of the longest chains was reached (mean square displacements greater than $R_{\rm e}^2$). At very low temperatures near $T_{\rm g}$ the dynamics was dramatically slowed down especially for long chains. In this case, the self diffusive regime of the whole matrix was not reached but it was possible to assess the diffusion of tracers shorter than host chains.

III. THEORY AND DEFINITIONS

A. MEAN-SQUARE DISPLACEMENTS

For a given diffusant of length N_i (either host or tracer), two mean squared displacements (MSD) are of particular significance to assess their translation dynamics over broad time scales t: the MSD of monomers, denoted $g_{0,i}$, and the MSD of the center of mass (CM), denoted $g_{3,i}$. They are defined as:

$$g_{0,\rm i}(t) = \frac{1}{n_{c,i} N_i} \sum_{k=1}^{n_{c,i}} \sum_{j=1}^{N_i} \left\langle [\mathbf{r}_{k,j}(t) - \mathbf{r}_{k,j}(0)]^2 \right\rangle \ , \qquad (3)$$

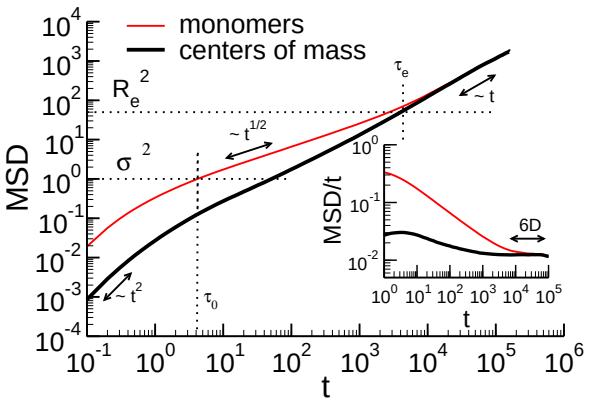

Figure 1: Main figure: MSDs of the monomers (thin line) and of the center of mass (thick line) of the chains for chain length $N = 32$ at $T = 1.0$. Intersection of the monomer's MSDs with horizontal dotted line σ gives τ_0 and intersection of chain's center of mass MSDs with dotted line $R_{\rm e}^2$ gives relaxation time $\tau_{\rm e}$. Inset: MSDs divided by time which give the long time diffusion coefficient D caracterized by a plateau regime in the figure.

and that of the chains center of mass (CM)

$$g_{3,\rm i}(t) = \frac{1}{n_{\rm c,i}} \sum_{k=1}^{n_{\rm c,i}} \left\langle [\mathbf{R}_k(t) - \mathbf{R}_k(0)]^2 \right\rangle \ , \qquad (4)$$

where $r_{k,j}$ is the position of the atom j in the kth diffusant of length N_i (total number of diffusants $= n_{c,i}$); $\mathbf{R}_k$ is the corresponding CM position. All positions were chosen relative to the mass reference frame of the whole system. For monodisperse systems there is only one species so $g_{0,i}$ and $g_{3,i}$ were denoted g_0, g_3.

A typical evolution of $g_{0,i}(t)$ and $g_{3,i}(t)$ is depicted in Figure 1 for a monodispersion of chains N=32 at T=1.0. On short time scales, monomers moved faster than compared to their CM center but were slowing down on intermediate time scales until to translate at a rate similar to their CM as soon as the displacements of their CM were uncorrelated. The successive scaling regimes are ballistic ($\propto t^2$), subdiffusive ($\propto t^{1/2}$) and finally diffusive ($\propto t$). On long term, the connectivity of chains enforces the equality:

$$g_0(t) \stackrel{t\to\infty}{=} g_3(t) \stackrel{t\to\infty}{=} 6Dt \ . \qquad (5)$$

Characteristic times, τ_0 and $\tau_{\rm e}$ identified in Figure 1, are determined when $g_{0,i}(t)$ equals σ^2 and $\tau_{\rm e}$ when $g_{3,i}(t)$ equals the diffusant square end-to-end distance.

B. ROUSE MODEL

The Rouse model was first introduced by P.E Rouse in 1953 [13] and was very successful to describe the dynamics of short non entangled homolinear chains. From

this theory, the relaxation modes so-called Rouse modes $\mathbf{X}_p(t)$ defined in Eq.(6) and their relaxation times (τ_p) can be expressed analytically.

$$\mathbf{X}_p(t) = \sqrt{\frac{2}{N}} \sum_{i=1}^{N} \mathbf{r}_i(t) \cos\left(\frac{(i-\frac{1}{2})p\pi}{N}\right) . \quad (6)$$

In addition, an expression $g_{0,i}(t)$ can be derived according to N_i. The model assumes ghost chains, which do not interact together and can freely cross over. Monomers are subjects to a local friction ξ_0 and to a random force. The corresponding equation of motion for a monomer i of the chain is:

$$\xi_0 \dot{\mathbf{r}}_i(t) = \mathbf{F}_i(t) - \frac{\partial}{\partial \mathbf{r}_i} U(\mathbf{r}_i) . \quad (7)$$

By assuming the solution of Equation (6) for the Rouse modes and inserting it in Equation (7) an expression for the Rouse time is obtained:

$$\tau_p = \frac{\xi_0(T,N) b^2}{12 k_B T} \left[\sin\frac{p\pi}{2N}\right]^{-2} . \quad (8)$$

By noticing that rouse modes are the cosine transform of atom positions, they can be back Fourier transformed to yield a practical expression of $g_0(t)$:

$$g_0(t) = 6\frac{k_B T}{N\xi_0(T)} t + 4\sum_{p=1}^{N} \langle X_p^2(0)\rangle \left[1 - \frac{\langle X_p(t) X_p(0)\rangle}{\langle X_p^2(0)\rangle}\right] . \quad (9)$$

The zero frequency component in Equation (9) is the most important as it predicts the asymptotic diffusion coefficient:

$$D = \frac{k_B T}{N\xi_0(T,N)} , \quad (10)$$

where $\xi_0(T,N)$ is the friction of a single monomer of the chain. In practice, the complete sampling of displacements spectrum is achieved when chain moves along a distance greater than its own end to end distance R_e^2 (see figure 1). This condition of ergodicity (chains have completely lost memories of their previous positions) is achieved for time scales $t > \tau_e$, where τ_e is defined as:

$$D = \frac{R_e^2}{6\tau_e} . \quad (11)$$

However for short chains it turns out that a larger distance than R_e^2 must be used. In the case of flexible chains, as for our bead-spring model, R_e^2 is roughly equals to

$$R_e^2 \simeq r_0^2 (N-1) , \quad (12)$$

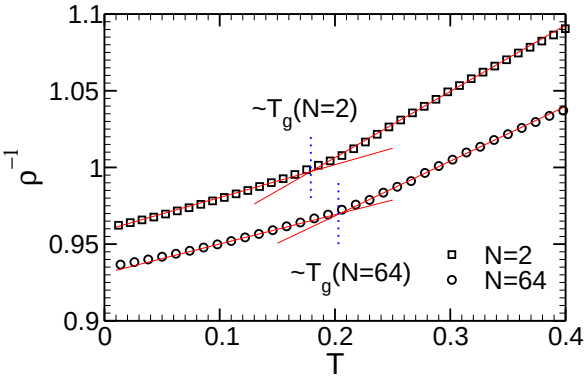

Figure 2: Inverse density of a monomer in function of the temperature for monodisperse $N = 2$ (squares) and $N = 64$ (circles) systems. The lines are fits of the liquid and solid branches for $N = 64$ and 2. The intersection of those lines determines the T_g of the system.

$$\tau_e = \frac{\xi_0(T,N) r_0^2 N(N-1)}{6 k_B T} = \tau_0(T,N) N(N-1) . \quad (13)$$

with τ_0 being the required time for a monomer to move a distance equals to its diameter $r_0^2 \simeq \sigma^2$.

IV. RESULTS AND DISCUSSION

This section details the results on both monodisperse and polydisperse systems at various temperatures. General dynamical properties of the matrix and diffusants are derived on monodisperse ones, as sampling statistics were improved with such systems. The similarities and discrepancies between self-diffusion and tracer diffusion of similar oligomers are analyzed separately.

A. GLASS TRANSITION OF MONODISPERSE SYSTEMS

The glass transition temperature T_g was derived from the variation of the specific volume, ρ^{-1}, as the temperature decreased. The results are plotted in Figure 2 for two extreme cases: $N = 2$ and $N = 64$. T_g was defined as intersection of straight lines on both sides the expected location limiting the glassy state and the liquid state. A satisfactory statistics was achieved by repeating cooling simulations. We fit the lower-T branch (glassy state) and the high-T branch (liquid state) over the largest possible range of temperature and take the same interval in temperature for both branches. The intersection of the straight lines gives the glass transition temperature T_g. However, the value depends slightly on the temperature region chosen for the fit hence it is difficult to obtain a rigorous T_g. To achieve a better statistical accuracy we repeated the cooling run $15n_c$ times.

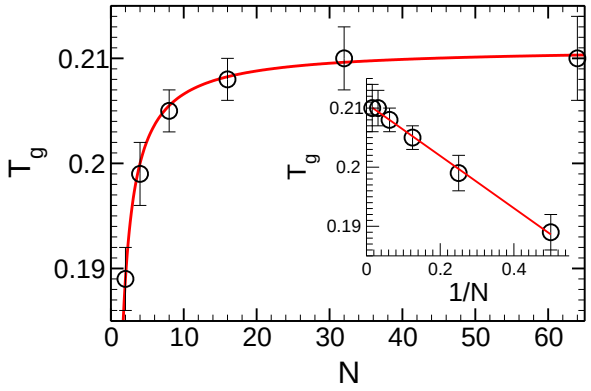

Figure 3: Glass transition temperature T_g as a function of the chain length N. The inset displays T_g as a function of $\frac{1}{N}$. The lines are a fit of data to equation (14).

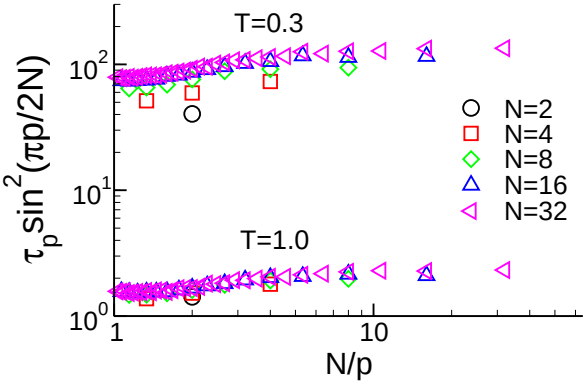

Figure 4: Rouse times τ_p multiplied by $\sin^2(\frac{p\pi}{2N})$ as a function of N/p. All monodisperse chain lengths are represented at $T = 1.0$ (lower part of the figure) and at $T = 0.3$ (upper part).

For our monodisperse samples the $\overline{T_g}$ reported is an average over n_c coolings ($n_c = 15$) associated with the error bar $\Sigma = \sqrt{\frac{1}{n_c}\sum_{i=1}^{n_c}[\overline{T_g} - T_g^i]^2}$. The chain length dependence on T_g was plotted in Figure 3. Error bars depict the standard deviation of the 15 determinations. T_g increased with N according to the following model (see the inset graph in Figure 2):

$$T_g = T_g^{\infty} - \frac{A}{N}\ , \qquad (14)$$

with $T_g^{\infty} \simeq 0.211$ and $A \simeq 0.044$.

B. ROUSE TIMES AND MSD OF MONODISPERSE SYSTEMS

In this section the Rouse times (τ_p) and the MSD determined from the theory and simulations were compared.

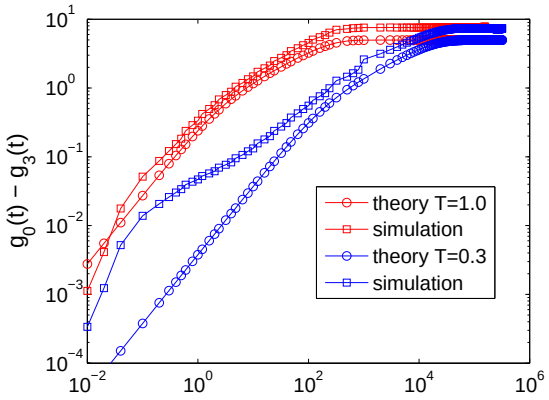

Figure 5: $g_0(t)$ - $g_3(t)$ determined theoretically and from simulations for $N = 16$ at $T = 1.0$ (upper curves) and $T = 0.3$ (lower curves).

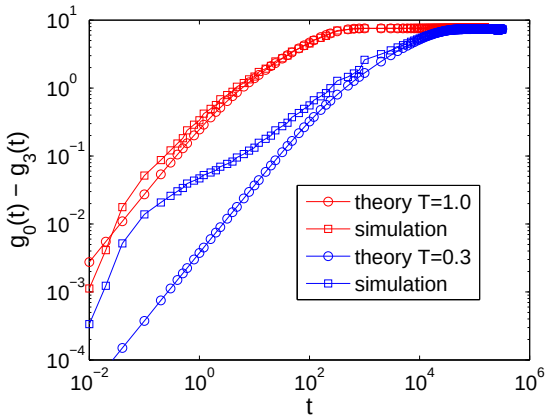

Figure 6: $g_0(t)$ - $g_3(t)$ obtained from simulation and from an approximation of the theory (see text) for $N = 16$ at $T = 1.0$ and at $T = 0.3$.

The theory provides an analytical expression for τ_p (see Eq(8)). The product of τ_p with $\sin^2(\frac{p\pi}{2N})$ should be a constant over the whole range of p modes. The result is ploted in Fig.4 for two extreme temperatures $T = 1.0$ and $T = 0.3$ for all the monodisperse chain lengths. For the same chain length the behavior is identical at the two temperatures. Three regions can be distinguished: at large p the product is constant, it slightly increases at intermediate modes and finally converges toward a constant at small p. There is approximately a factor of two between the values of the two invariant regions. At $T = 1.0$ the different chain lengths are well superimposing but not at $T = 0.3$ especially for short chains. These discrepancies are assumed to be due to the friction coefficient $\xi_0(T, N)$.

MSD were compared using the second term of equation (9) which is identical to $g_0(t) - g_3(t)$. Figure 5 shows this quantity for chain $N = 16$ at $T = 1.0$ and

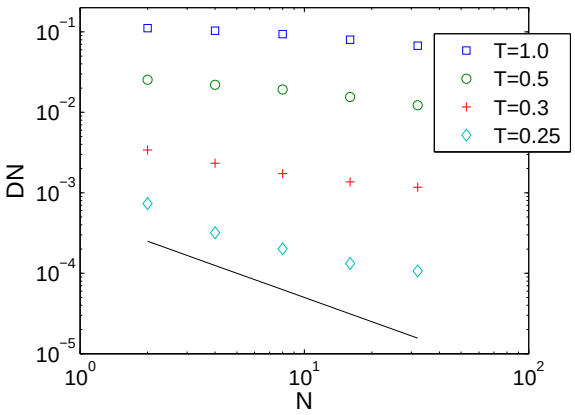

Figure 7: DN as a function of N for all the self-diffusing chains at $T = 1.0, 0.5$ and 0.25. The black line $(1/N)$ is a guide to the eyes.

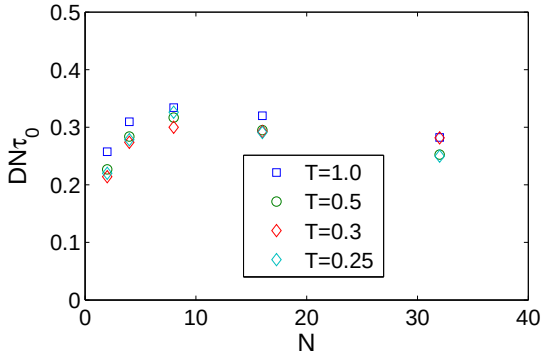

Figure 8: $DN\tau_0$ as a function of N for temperatures $T = 1.0$ to 0.25.

0.3. $\langle X_p(t)X_p(0)\rangle$ and $\langle X_p(0)^2\rangle$ were determined theoretically and from simulations. In both cases the theory reproduces very well the sub-diffusive regime. However neither the ballistic regime at $T = 1.0; 0.3$ nor the slowing down due to the cage at $T = 0.3$ were predicted. Furthermore the theoretical converged value of $g_0(t) - g_3(t)$ was smaller than the simulated one. As an approximation of the theory $\langle X_p(0)^2\rangle$ determined from simulations were injected in the model as displayed in Fig.6. In this case the Rouse theory gave a really good description of the simulation for the sub-diffusive regime at both temperatures.

C. DIFFUSION COEFFICIENTS OF MONODISPERSE SYSTEMS

Self-diffusion coefficients were derived either from relaxation times τ_e or from the rate of increase of the $g_{i,3}$ with time during the asymptotic regime. Both estimates of D are in good agreement and scaled with N_i with an exponent α depending on the temperature as:

$$D \propto \frac{1}{N^{\alpha(T)}} \, . \tag{15}$$

Figure 7 shows D multiplied by N as a function of N at different temperatures. The exponent α was found to vary from $\alpha \simeq 1$ at $T = 1.0$ to $\simeq 1.8$ at $T = 0.25$.

We also indentified that D could be estimated from the typical time τ_0 defined in equation (13). This feature was particularly outstanding as the monomoric relaxation was much faster than the whole chain so that asymptotic self diffusion coefficient could be approximated from short terms molecular dynamics simulations. To follow the Rouse prediction for the long term diffusion coefficient of Eq.(9) it was assumed that

$$DN \propto \frac{1}{\tau_0} \, . \tag{16}$$

Here τ_0 was proportional to the monomeric friction coefficient (see Eq.(13)). The influence of the latter on the exponent $\alpha(T)$ was assessed according to equation(16). Figure 8 displays $DN\tau_0$ as a function of N and for different temperatures. The data points almost superimposed for all temperatures and are nearly independent of the chain length. This feature was quite remarkable as:

$$D(T)\tau_0(T) \propto \frac{1}{N^{\alpha}} \, , \tag{17}$$

where α was approximately equal to 1 when the chains were neither too short nor too long. This result agreed with the Rouse theory for the dependence of D on N. Furthermore all temperature dependence of D seemed controlled by τ_0.

The evolution of D with T for $N = 16$ is shown in Figure 9 as an Arrhenius plot for temperatures ranging from 0.23 to 1. A straight line was approximately obtained in the high-T region (from $T = 1$ to 0.4). Near T_g , a significant deviation to an Arrehnian behavior is observed. For the whole temperature range, the evolution was better described by an expression from mode coupling theory (MCT). All data are appropriately fitted except the last one point at $T = 0.23$ for which a D value greater than the theory was predicted. Further insight on deviations to theory was obtained by plotting in Figure 11 the variation evolution of D scaled with N against the renormalized temperature $T/T_g(N)$ (Figure 11). Two master curves defined by MCT theory and a modified Arrehenius expression equation (18) were generated for chain lengths from $N = 2$ to 32. Except for chains longer than 16, the deviation to MCT model was not significant. By contrast for $N = 32$, the simulated data were systematically underneath the master curve. As a result, it was argued that topological constraints tended to dominate so that the system shifted gradually

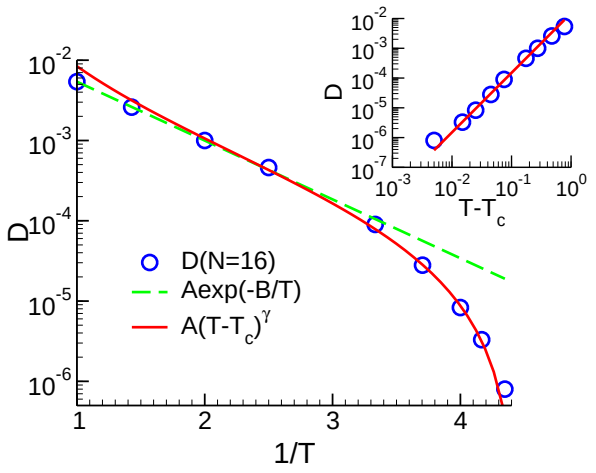

Figure 9: Main figure: Arrhenius representation of the evolution of the diffusion coefficient with temperature for $N = 16$ chains (circles). Temperature goes from 1 to 0.23. The dashed line is a fit to Arrhenius law of the high-T region and lines are MCT fit of the low-T region. Inset: diffusion coefficient as a function of T rescales by the MCT temperature T_c.

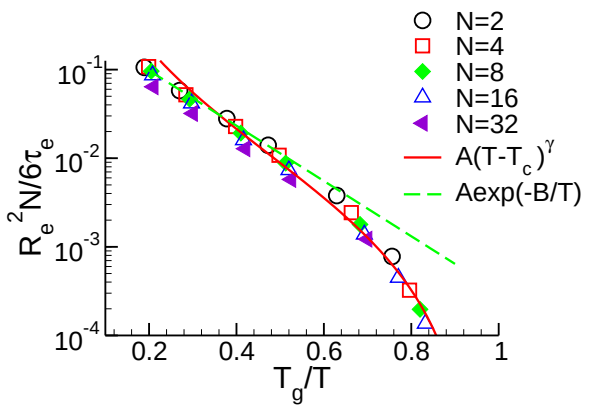

Figure 10: Arrhenius representation of D obtained from τ_e for the different chain lengths but rescaled by Tg. Thus we plot D in a logarithmic scale along y axis and T_g/T along the x axis. The dashed line is an Arrhenius law's fit to our data and the line is a MCT fit of the data for lower temperatures.

with N from a pure Rouse regime towards a reptation one. Besides, the modified Arrhenius equation defines in (15) provides an acceptable estimate for $T > 0.6\ T_g$ and in particular better than Eq.(11).

$$D = \frac{A}{N} \exp\left(-\frac{BT_g(N)}{T}\right) . \qquad (18)$$

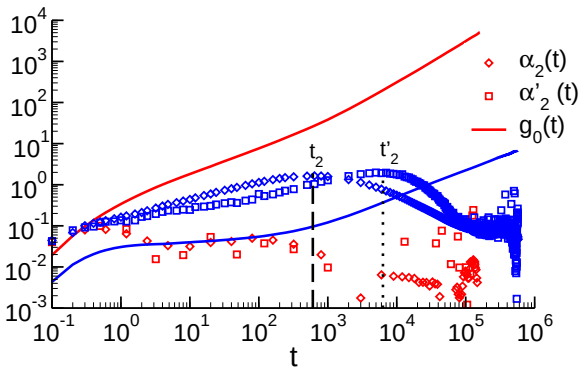

Figure 11: Non-Gaussian parameter $\alpha_2(t)$ (diamonds), modified non-Gaussian parameter $\alpha'_2(t)$ (squares) and monomer's MSD (lines) at temperatures $T = 1.0$ (light colour) and $T = 0.23$ (deep colour). The vertical dashed and dotted black lines indicate respectively peak times t and t' of $\alpha_2(t)$ and $\alpha_2(t')$.

D. HETEROGENEOUS DYNAMICS NEAR T_g

As temperature approaches T_g, many studies suggest that the dynamics becomes heterogeneous. This behavior was assessed by studying the quartic moments of the displacements, using the following non-Gaussian parameters:

$$\alpha_2(t) = \frac{3}{5g_0(t)^2} \frac{1}{N_p} \sum_{i=1}^{N_p} \langle |\mathbf{r}_i(t) - \mathbf{r}_i(0)|^4 \rangle - 1 . \qquad (19)$$

In complement to α_2 we use a modified non-Gaussian parameter introduced in [4] defined as:

$$\alpha'_2(t) = \frac{g_0(t)}{3} \frac{1}{N_p} \sum_{i=1}^{N_p} \left\langle \frac{1}{|\mathbf{r}_i(t) - \mathbf{r}_i(0)|^2} \right\rangle - 1 . \qquad (20)$$

When displacements are sufficiently independent on time period t, quartic moments (19,20) vanish. Positive values identify distribution tails that are are thicker than the Gaussian one and in particular attest the mixing of fast and slow displacements. Non-Gaussian parameters and $g_0(t)$ are plotted in Figure 12 for the monodisperse system $N = 16$ at two different temperatures $T = 1.0$ ($>> T_g$) and $T = 0.23$ (close to T_g). At high temperature, non-Gaussian parameters remained very small over all time scales. The succession of ballistic, sub-diffusive and diffusive regimes was well identified on g_0 as already described in figure 1. Near T_g , $g_0(t)$ exhibited a plateau sub-diffusive regime following the short-time ballistic regime. Non-gaussian parameters were significant and confirmed the presence of correlated displacements, which were responsible of the dramatic slowdown of monomers motions. As an illustration, one monomer required 4τ to translate beyond its size at $T = 1.0$

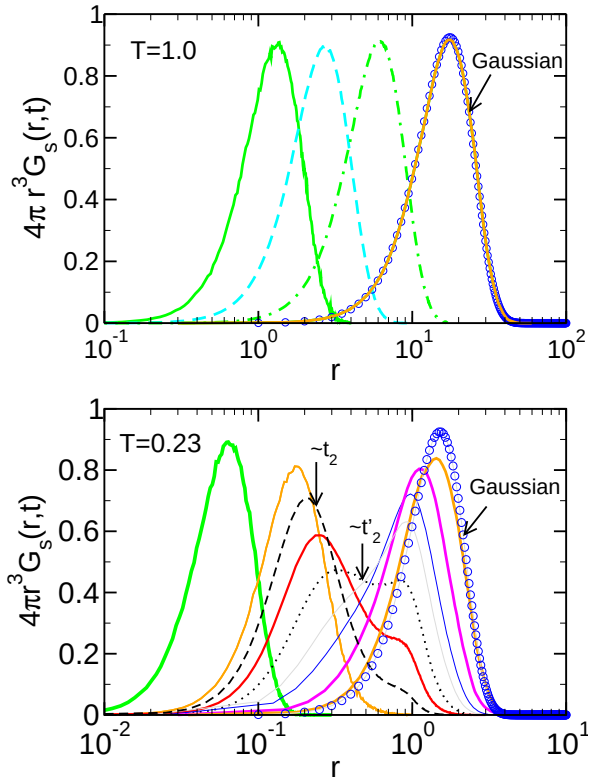

Figure 12: Upper panel: Probability distributions functions at high temperature for times $t = 10, 100, 1000, 10000$ (from the left to the right) for chain length $N = 16$. For the last time we also drew in grey circles the theoretical expression of the gaussian. Lower panel: Probability distributions functions at $T = 0.23$ for times $t = 0.1, 10, 600, 2500, 6000, 10000, 25000, 50000, 100000$.

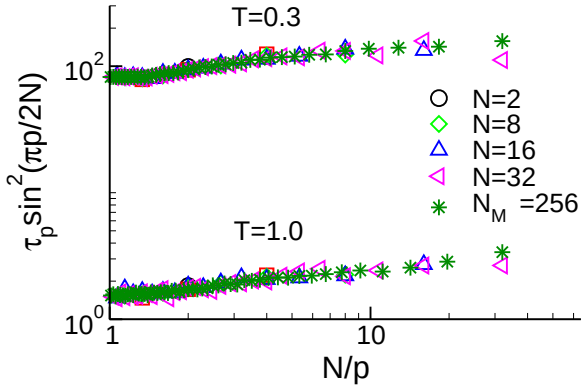

Figure 13: Rouse times τ_p multiplied by $\sin^2 \frac{p\pi}{2N}$ for all the tracer chain lengths and the matrix at temperatures $T = 1.0$ and $T = 0.3$.

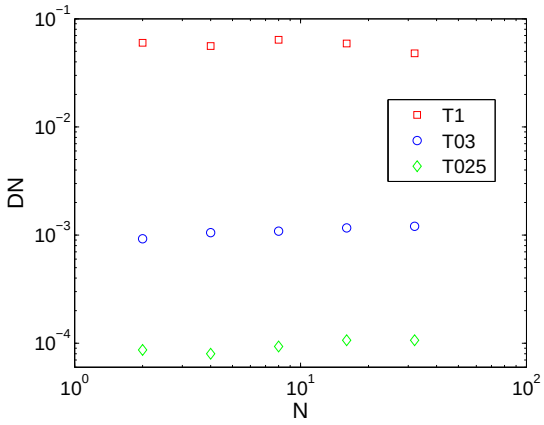

Figure 14: Diffusion coefficient of the tracers as a fonction of N for temperatures $T = 1.0$ down to $T = 0.25$.

whereas 22000τ was needed at $T = 0.23$. A detailed analysis of displacements was performed by calculating the radial distribution function $P(r;t)$. The latter is related to the self part of the van-Hove correlation function $G_s(r,t)$ by:

$$P(\ln r; t) = 4\pi r^3 G_s(\ln r, t) \ , \tag{21}$$

and

$$G_s(\mathbf{r}, t) = \frac{1}{N_p} \sum_{i=1}^{N_p} \langle \delta([\mathbf{r}_i(t) - \mathbf{r}_i(0)] - \mathbf{r}) \rangle \ . \tag{22}$$

$G_s(r,t)$ is plotted on a semi-log scale in figure 13 for the monodisperse chain length $N = 16$ at $T = 1.0$ and $T = 0.23$. The theoretical distribution corresponding to a Gaussian with zero mean and a variance equal to $g_0(t)$ is also represented. The Gaussian shape was well verified at high temperatures and at all time scales. By contrast at $T = 0.23$, a second mode is identified on intermediate time scales ($t \simeq t_2$). The second mode position coincided with a monomer diameter. At the particular time scale ($t \simeq t'_2$), both modes were equal, suggesting two independent populations: a caged one and a movable one beyond a bead diameter as described in [4][12]. For $t > t'_2$, the caged population vanished progressively (trapped beads started to move freely) and the long term distribution converged finally towards a true Gaussian.

V. EXTENTION TO TRACER DIFFUSION OF OLIGOMERS IN LONGER CHAIN MATRICES

Multiconstiuents mixtures consisted in a matrix of long chains mixes with smaller chains. Two types of configurations were tested: bidisperse ones with only a single tracer and polydisperse systems with several tracers of different chain lengths. Bidisperse systems were mainly used to verify that the presence of tracers dit not influence the matrix relaxation and structure factor. While their overall concentration remained low, polydisperse systems contributed to reduce the computational effort

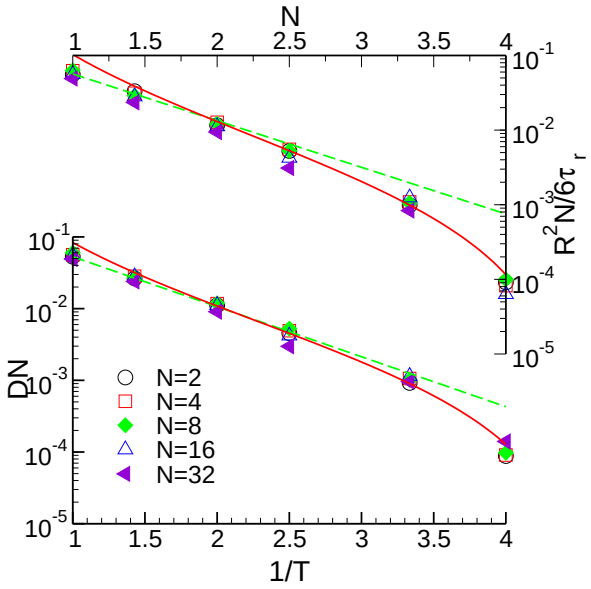

Figure 15: Arrhenius representation of the evolution of the diffusion coefficient of tracers in $N_{\rm M} = 256$ matrix with the temperature. Upper panel: D obtained from relaxation time $\tau_{\rm e}$. Lower panel: D we determined from the MSDs. The dashed lines are Arrhenius laws fits for the high-T region and lines represent MCTs fits for lower temperatures.

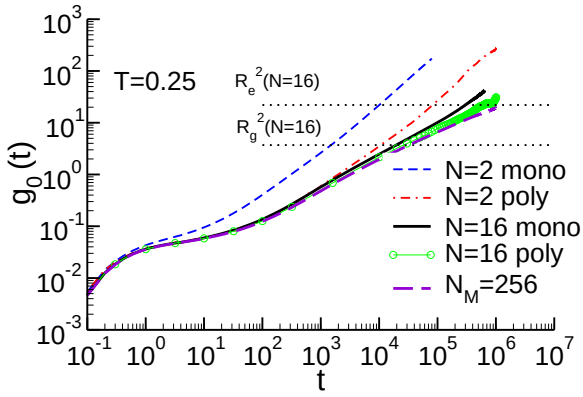

Figure 16: Monomer's MSDs g_0 of monodisperse $N = 2, 16$ chains and polydisperse ones at $T = 0.25$. The horizontal dotted lines are $R_{\rm e}^2$ and $R_{\rm g}^2$ of $N = 16$ chains.

for a large cohort of tracers diffusants. Similarly, $T_{\rm g}$ was extrapolated from Eq.(14) to 0.211.

Following the self-sytems study (see Part "Rouse times and MSD of monodisperse systems") the Rouse theory was compared to simulations for the Rouse times multiplied by $\sin^2 \frac{p\pi}{2N}$ in figure 14. Same observations as in monodisperse systems were made for one chain length. However in the polydisperse case all the different chain lengths are superimposing with the matrix curve at all temperatures.

The MSD derived from the theory were also examined

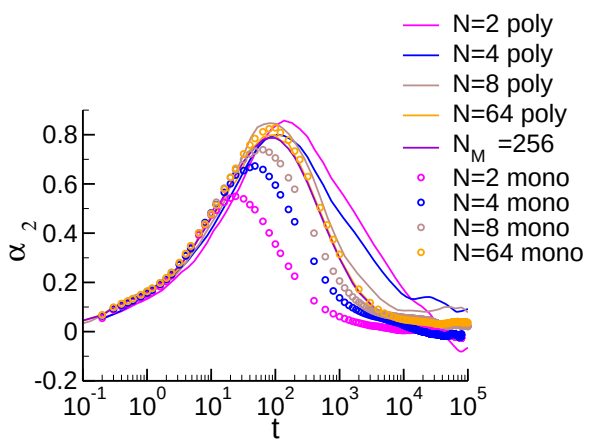

Figure 17: Non-Gaussian parameter $\alpha_2(t)$ at $T = 0.25$ for $N = 2, 4, 8, 64$ monodisperse chains represented by the symbols and for tracers $N = 2, 4, 8, 64$ in the polydisperse system symbolised by lines.

for $N = 16$ at $T = 1.0$ and $T = 0.25$ but no divergence with the self counterpart was found.

Tracer diffusion coefficients were obtained in a similar fashion as self-diffusion coefficients, from either MSD or relaxation times (see Eq.(11)):

$$D = \frac{R^2}{6\tau_{\rm R}}\,, \tag{23}$$

where $\tau_{\rm R} = 3\tau_{\rm e}$ and R^2 denotes the MSD of the chain center of mass at $\tau_{\rm R}$. The introduced safety margin in via $\tau_{\rm R}$ ensured D values determined from the rate of increase of MSDs with time-scale. Estimated tracer diffusion coefficients scale with chain length are displayed as an Arrhenius plot in Figure 16. The chain length dependence was in good agreement with the Rouse exponent $\alpha = 1$ over the whole range of studied temperatures as shown in figure 15. This result was particularly outstanding as it differs from monodisperse systems where a temperature dependence of α was observed. For the high-T region (T ranged between 1.0 to 0.4) D followed an Arrhenius law whereas a MCT law was found more appropriated at lower temperatures near $T_{\rm g}$. The results demonstrated that the asymptotic translation mechanisms associated to the tracer diffusion among long chains and the one associated to its self diffusion counterpart were very similar. Nevertheless, the tracer diffusion coefficients were much slower for the polydisperse case especially for very short chains and any temperature dependence of the exponent α was noticed. This behavior was related to the relaxation time τ_0 value which was governed by the matrix dynamics.

The coupling between the host relaxation and tracer diffusion is illustrated in Figure 17 by plotting monomer's MSDs of chains $N = 2$ and 16 at $T = 0.25$ for both monodisperse and polydisperse ($N_{\rm M} = 256$) systems. For

the polydisperse systems, a short plateau regime for $t \simeq 1$ to $\simeq 30$ was clearly visible and confirmed that the whole system was close to its T_g. On intermediate time scales, it is worth to notice that MSD for $N = 16$ chains were not distinguishable between monodisperse and polydisperse systems. A separation occurred only after $g_0 = R_g^2$ as the chain relaxation (τ_e) occured earlier in the monodisperse case and MSDs of $N = 16$. For very short tracer lengths, the influence of the matrix was stronger. In the special case of $N = 2$ the two systems separated immediately after the ballistic regime.

The comparison between monodisperse and polydisperse systems is completed in Figure 18 by the evolution of the non-Gaussian parameter α_2 Eq.(19) with time scale at $T = 0.25$ for $N = 2, 4, 8, 64$. Increasing the chain length translated in time the non-Gaussian behavior in monodisperse systems, while it had no effect in polydisperse systems. These results confirmed the crucial role of the host matrix on the dynamics of tracer on short and intermediated time scales.

VI. CONCLUSION

In this paper we presented results obtained from molecular dynamics simulations on the diffusion of small chains in monodisperse systems and in an entangled matrix. We first analysed monodisperse systems. We compared three different ways of calculating the diffusion coefficient. The first one from the mean-square displacements divided by time, second from the monomer relaxation time (τ_0) and last from the relaxation of the polymer chain (τ_e). We found a good agreement between the different methods used to evaluate D and therefore there is a correspondence between the local mobility (τ_0) and that of the chain (τ_e). This implies that motion of monomers are uncorrelated from one another. This leads to a Rouse description of the dynamics. To support this interpretation we tested the power law dependence of the diffusion coefficient on chain length $D \propto N^{-\alpha}$ and found the Rouse exponent $\alpha = 1$ with corrections for very short chains ($N \leq 4$) because gaussianity is not verified and for very long chains ($N \geq 32$) because entanglements start to play a role. We saw that the dependence of D with the temperature for very high T, $T \geq 2T_g$, is given by an Ahrrenius law $A \exp\left(-\frac{B}{T}\right)$. For lower temperatures until close to T_g D is well described by an expression derived from MCT, $D = A(T - T_c)^\gamma$. This relation breaks down very close to T_g. It predicts a divergence of the relaxation time at T_c and a vanishing of D that is not observed neither experimentally nor in our simulations. Following previous study [4] we paid special attention to the change of dynamics occuring near T_g. At high temperatures we saw that the distribution of displacement is Gaussian at all times which implies a continuous diffusion whereas at low temperatures there is an intermediate time regime for which the distribution of displacements differs from a Gaussian. At this intermediate time regime some parts of the system have an enhanced mobility. In a general manner particles remain trapped by their surronding and it takes a long time for a particle to move. After this study of monodisperse systems we analyzed tracers diffusion that is short chains in very low concentration diffusing inside a matrix of long chains. We called those systems polydisperse. We compared the different methods to obtain the diffusion coefficient and found in this case the different methods are not in agreement with one another. This comes from the fact that we arbitrarly decided of the relaxation time τ_e that is when the chain moved a distance of its end-to-end squared distance. By taking $3\tau_e$ we might find the good value of the diffusion coefficient. We evaluated the dependence of the tracers diffusion coefficients on the temperature and chain length. We found that as in the monodisperse case the dependence of the diffusion coefficient on the chain length is still given by the Rouse exponent $\alpha = 1$ for $D \propto N^{-\alpha}$. The dependence with the temperature for very high temperatures $T \geq 2T_g$ is also following an Arrhenius law. Howewer the dynamic of oligomers chains is slower than for the monodisperse systems. It is because the local mobility is governed by the matrix which increases the monomer relaxtion time but the displacements of monomers are still uncorrelated with one an other and therefore it leads to a Rouse description of the diffusion. For the flexible model the confinment imposed by the matrix on the oligomers is not strong enough such that it limits tranverse displacements. Future works will consist in increasing the constraints on the matrix so as to rigidify the system and limit the transverse motions of monomers. This can be done by adding angular constraints and also torsional constraints. A particular attention is paid to semi-crystalline systems because there are ordered regions that hindered oligomers diffusion and influence the segmental mobility of amorphous regions. It could leads to a different scaling exponent of diffusants diffusion with N.

[1] LA Deschenes and DAV Bout, *Molecular motions in polymer films near the glass transition: a single molecule study of rotational dynamics*, JOURNAL OF PHYSICAL CHEMISTRY B **105** (2001), no. 48, 11978–11985.

[2] LA Deschenes and DA Vanden Bout, *Single-molecule studies of heterogeneous dynamics in polymer melts near the class transition (Retracted article. See vol 312, pg 195, 2006)*, SCIENCE **292** (2001), no. 5515, 255–258.

[3] M DOI, *EXPLANATION FOR THE 3.4-POWER LAW FOR VISCOSITY OF POLYMERIC LIQUIDS ON THE BASIS OF THE TUBE MODEL*, JOURNAL OF POLYMER SCIENCE PART B-POLYMER PHYSICS **21** (1983), no. 5, 667–684.

[4] E Flenner and G Szamel, *Relaxation in a glassy binary*

mixture: Mode-coupling-like power laws, dynamic heterogeneity, and a new non-Gaussian parameter, PHYSICAL REVIEW E **72** (2005), no. 1, Part 1 (English).

[5] VA Harmandaris, M Doxastakis, VG Mavrantzas, and DN Theodorou, *Detailed molecular dynamics simulation of the self-diffusion of n-alkane and cis-1,4 polyisoprene oligomer melts*, JOURNAL OF CHEMICAL PHYSICS **116** (2002), no. 1, 436–446 (English).

[6] VA Harmandaris, VG Mavrantzas, DN Theodorou, M Kroger, J Ramirez, HC Ottinger, and D Vlassopoulos, *Crossover from the rouse to the entangled polymer melt regime: Signals from long, detailed atomistic molecular dynamics simulations, supported by rheological experiments*, MACROMOLECULES **36** (2003), no. 4, 1376–1387 (English).

[7] K. Kremer and G. S. Grest, *Dynamics of entangled linear polymer melts: a molecular-dynamics simulation.*, J. Chem. Phys. **92** (1990), no. 8, 5057–86.

[8] KS Kwan, CNP Subramaniam, and TC Ward, *Effect of penetrant size and shape on its transport through a thermoset adhesive: I. n-alkanes*, POLYMER **44** (2003), no. 10, 3061–3069.

[9] Jerome Lezervant, Olivier Vitrac, and Alexandre Feigenbaum, *Multiscale determination of diffusive properties in polymers: Application to the prediction of desorption packaging constituents into foodstuffs*, FOODSIM '2006: 4TH INTERNATIONAL CONFERENCE ON SIMULATION AND MODELLING IN THE FOOD AND BIO-INDUSTRY (Masi, P and Toraldo, G, ed.), 2006, 4th International Conference on Simulation and Modelling in the Food and Bio Industry (FOODSIM 2006), Naples, ITALY, JUN 15-17, 2006, pp. 75–79.

[10] Timothy P. Lodge, *Reconciliation of the molecular weight dependence of diffusion and viscosity in entangled polymers*, Physical Review Letters **83** (1999), 16.

[11] F. R. Blackburn Marcus T. Cicerone and M. D. Ediger, *Anomalous diffusion of probe molecules in polystyrene: Evidence for spatially heterogeneous segmental dynamics*, Macromolecules **28** (1995), 8224.

[12] S. Peter, H. Meyer, and J. Baschnagel, *Molecular dynamics simulations of concentrated polymer solutions in thin film geometry. I. Equilibrium properties near the glass transition*, JOURNAL OF CHEMICAL PHYSICS **131** (2009), no. 1.

[13] Prince E. Rouse, *A theory of the linear viscoelastic properties of dilute solutions of coiling polymers*, Journal of chemical Physics **21** (1953), 1272.

[14] O. Vitrac and M. Hayert, *Effect of the distribution of sorption sites on transport diffusivities: A contribution to the transport of medium-weight-molecules in polymeric materials*, CHEMICAL ENGINEERING SCIENCE **62** (2007), no. 9, 2503–2521.

[15] O. Vitrac, A. Mougharbel, and A. Feigenbaum, *Interfacial mass transport properties which control the migration of packaging constituents into foodstuffs*, JOURNAL OF FOOD ENGINEERING **79** (2007), no. 3, 1048–1064.

[16] Olivier Vitrac and Jean-Charles Leblanc, *Consumer exposure to substances in plastic packaging. I. Assessment of the contribution of styrene from yogurt pots*, FOOD ADDITIVES AND CONTAMINANTS **24** (2007), no. 2, 194–215.

[17] Olivier Vitrac, Jérôme Lézervant, and Alexander Feigenbaum, *Decision trees as applied to the robust estimation of diffusion coefficients in polyolefins*, Journal of Applied Polymer Science **101** (2005), 2167.

[18] E. von Meerwall and S. Beckman, *Diffusion of liquid n-alkanes: Free-volume and density effects*, Journal of chemical Physics **108** (1998), 4299.

[19] Ernst D. von Meerwall, Heng Lin, and Wayne L. Mattice, *Trace diffusion of alkanes in polyethylene: Spin-echo experiment and Monte Carlo simulation*, MACROMOLECULES **40** (2007), no. 6, 2002–2007 (English).

[20] M Zamponi, A Wischnewski, M Monkenbusch, L Willner, D Richter, AE Likhtman, G Kali, and B Farago, *Molecular observation of constraint release in polymer melts*, PHYSICAL REVIEW LETTERS **96** (2006), no. 23.